Determining Energy Expenditure from Treadmill Walking using Hip-Worn Inertial Sensors: An Experimental Study

Harshvardhan Vathsangam, Adar Emken, E. Todd Schroeder, Donna Spruijt-Metz and Gaurav S. Sukhatme

***Abstract*—We describe an experimental study to estimate energy expenditure during treadmill walking using a single hip-mounted inertial sensor (triaxial accelerometer and triaxial gyroscope). Typical physical activity characterization using commercial monitors use proprietary counts that do not have a physically interpretable meaning. This paper emphasizes the role of probabilistic techniques in conjunction with inertial data modeling to accurately predict energy expenditure for steady-state treadmill walking. We represent the cyclic nature of walking with a Fourier transform and show how to map this representation to energy expenditure ($\dot{V}O_2$, mL/min) using three regression techniques. A comparative analysis of the accuracy of sensor streams in predicting energy expenditure reveals that using triaxial information leads to more accurate energy expenditure prediction compared to only using one axis. Combining accelerometer and gyroscopic information leads to improved accuracy compared to using either sensor alone. Nonlinear regression methods showed better prediction accuracy compared to linear methods but required an order of higher magnitude of run time.**

***Index Terms*—Accelerometer, Energy expenditure, Gyroscope, Treadmill walking**

I. Introduction

Physical inactivity is the fourth leading risk factor for global mortality (6% of global deaths) and is estimated to be the main cause of approximately 21–25% of breast and colon cancers, 27% of diabetes and approximately 30% of ischaemic heart disease burden [1]. Regular physical activity is known to reduce obesity, risks for cardiovascular disease, type 2 diabetes, and several forms of cancer [2]. In the quest to promote healthier lifestyles, technological solutions provide users and clinicians with objective measures of activity intensity that can be used in feedback and interventions. The challenge is to provide these tools in real-time and in portable form.

In recent years, considerable research has been directed towards the detection and classification of physical activity patterns from body mounted kinematic sensors [3]. Inertial sensors capture movement either by measuring body accelerations (accelerometers) or rotational rates (gyroscopes). Due to their small size, low cost, increasingly high precision, low power consumption and portability, inertial sensors are an attractive option for deriving relevant physiological quantities from human movement [4].

Energy expenditure prediction in walking: Walking is an easy and common activity that can be used to maintain an active lifestyle [5]. An objective measure of the intensity of walk is the energy expended. An immediate question to ask is whether body-worn inertial measurements can be exploited to predict energy expenditure. Can these predictions be improved with sophisticated analytical techniques? Finally, which kinds and combonations of sensors are better at predicting energy expenditure?

The domain: Here, we address the problem of estimating energy expenditure using body-mounted inertial sensors for a particular activity: treadmill walking. Treadmill walking was chosen because it allows the capture of a regular, well-defined and easily quantifiable movement in a laboratory setting. We use inertial data from a triaxial accelerometer and triaxial gyroscope mounted on the right iliac crest as inputs. We treat the functional mapping of these inputs to energy expenditure as a regression problem. Our approach to estimating energy expenditure from walking involves developing a probabilistic map from movement features to calories burned. A preliminary version of this paper appeared in [6].

II. Related Work

Much of the research involving using inertial sensors to calculate energy expenditure for daily activities has focused on the utility of accelerometers alone [7, 8]. There is a significant amount of work in using accelerometer-based commercial activity monitors to predict energy expenditure in a variety of settings [9]. A major drawback in using commercial activity monitors is imprecision. Imprecision arises because these monitors use proprietary methods to convert linear accelerations into epoch-based "counts" that are converted to caloric expenditure [10, 11, 12, 13]. The usage of counts is not meaningful or physically interpretable [14]. Some accelerometry-based techniques fit regression equations that map counts to energy expenditure [15, 16]. Standard linear regression does not explicitly address the significance of differing amounts of data available to derive model parameters. Single variable linear regression models are limited in that regression mapping to energy can be made richer by considering multi-dimensional features simultaneously [9]. An alternative approach to characterizing human motion involves pattern recognition techniques that extract meaningful properties or features from raw movement data and map these properties to calories expended [17]. These include neural networks [18], probabilistic linear regression [6] and piecewise regression [19]. Using such techniques, it is possible to "learn" a personalized model for each user from data collected. Access to raw data allows the

Revised version submitted April 30, 2011.

This work was supported in part by Qualcomm, Nokia, NSF (CCR-0120778) as part of the Center for Embedded Network Sensing (CENS), and the USC Comprehensive NCMHD Research Center of Excellence (P60 MD 002254). Support for H. Vathsangam was provided by the USC Annenberg Doctoral fellowship program.

H. Vathsangam and G. S. Sukhatme are with the Department of Computer Science, University of Southern California, Los Angeles, CA 90089. vathsang | gaurav @ usc.edu

A. Emken and D. Spruijt-Metz are with the Department of Preventive Medicine, University of Southern California, Los Angeles, CA 90089. emken | dmetz @ usc.edu

E.T. Schroeder is with the Division of Biokinesiology and Physical Therapy, University of Southern California, Los Angeles, CA 90089. eschroed@usc.edu

researcher to explore the physical intuition behind movement and use features that explicitly mirror the quantity in question.

Using accelerometry-only techniques suffers from a second limitation: incompleteness. The assumption behind using accelerometry for physical activity monitoring is that data from an accelerometer represents body movement [20]. However, rigid body movement consists of both accelerations and rotations [21]. Rotational data cannot be completely separated from translational data using a single triaxial accelerometer [22]. Current count-based accelerometry completely ignores rotational rates. Combining accelerometry and rotational rate measurements through gyroscopes would thus be a valuable tool in completely characterizing movement. Gyroscopes are not influenced by gravitational acceleration and are more displacement tolerant than accelerometers. This is because for a given body segment movement, a gyroscope provides the same readings irrespective of position as long as the axis of placement is parallel to the measured axis [3]. The introduction of low-cost, single-chip triaxial gyroscopic sensors [23] has introduced the possibility of using gyroscopes as alternatives to or in combination with accelerometers for activity characterization.

III. Analysis of Treadmill Walking Inertial Data

A. Periodicity of Human Walk

Steady state walking is cyclic [24, 21].This inherent periodicity was captured with inertial sensor data from the right iliac crest. Movement signals corresponded directly to the accelerations and rotational rates of the hip as measured by the sensor in its local frame of reference. Fig. 1a shows sample inertial data from treadmill walking collected over 10 seconds when a participant is walking at a speed of 2.5 mph. Regular periodic patterns were observed in steady-state. Similar patterns were observed for other speeds.

B. Variation of Periodicity with Speed

The periodicity of walking signals was examined by computing their Fourier transforms. Figure 1b illustrates Fourier transforms of two 10 second steady state walking samples at 2.5 mph and 3.5 mph for the X-axis acceleration streams. The Fourier transform showed clear peaks indicating distinct periodic components for the original signals. The peaks occurred at the same frequencies for all other sensor streams. The location of these peaks was a function of walking speed. The dominant peak for walking at 3.5 mph occurs at a higher frequency than the corresponding peak for walking at 2.5 mph. In prior work, the relationship between energy expenditure and walking speed has been modeled as one where walking at higher speeds requires higher energy expenditure [25, 26, 27]. The fact that each speed exhibits a characteristic frequency spectrum and that there exists a map between speed and energy expenditure suggests that one can track calories expended in treadmill walking using the frequency spectrum as a representative feature space.

IV. Mapping Walking Data to Energy Expenditure

A. Problem Formulation

Given the representation of treadmill walking using features described in Sec. III, we focused on the problem of deriving a mapping from these features to energy consumed as measured by VO_2 consumption (mL/min). We frame this as a regression problem. Consider a D-dimensional *input variable* $\mathbf{x} \in \mathbb{R}^D$ of which there are specific data points $\{x_n\}_{n=1}^N$. The goal of regression is to predict the value of one or more continuous *target variables* $\mathbf{t}$ of which there are corresponding observed values $\{t_n\}_{n=1}^N$ that are related to the input variables by a "best-fit" function $f(x_n)$. This section examines three candidate algorithms to find this map. We provide descriptions of each algorithm for the case of an arbitrary D-dimensional input variable and one dimensional target variable and discuss the relative merits and demerits of each.

B. Least Squares Linear Regression

Least Squares Regression (LSR) [28] models regression as a linear combination of input variables. Specifically, for an input data point $\mathbf{x}_n$, we have

$$\begin{aligned} t_n &= w_0 + w_1\phi_1(x_n) + \dots w_{M-1}\phi_{M-1}(x_n) + \epsilon \\ with\ \epsilon &\sim \mathcal{N}\left(\mathbf{0}, \beta^{-1}\mathbf{I}\right) \\ \implies t_n &= \mathbf{w}^T\phi(x_n) + \epsilon, \epsilon \sim \mathcal{N}\left(\mathbf{0}, \beta^{-1}\mathbf{I}\right) \end{aligned} \quad (1)$$

where ϵ is a noise parameter, $\phi = (\phi_0, \dots \phi_{M-1})^T$ is the derived function space consisting of fixed nonlinear functions of the input variables of dimension $M-1$ and $\mathbf{w} = (w_0, \dots, w_{M-1})^T$ are the weights . This model is linear in ϕ. This allows the usage of feature functions $\{\phi_j(x_n)\}$ derived from input variables x_n. Equation 1 describes a mapping from feature space $\{\phi_j(\mathbf{x}_n)\}$ to the output values t_n. Given that ϵ is a Gaussian, allowing a probabilistic interpretation, we have:

$$p(t_n|x_n, \mathbf{w}, \beta) = \mathcal{N}\left(t_n; \mathbf{w}^T\phi(x_n), \beta^{-1}\right) \quad (2)$$

We define an optimal fitting function as one that maximizes the likelihood $p(\mathbf{t}|\mathbf{w}^T\mathbf{X}) = \prod_{n=1}^{N} p(t_n|x_n, \mathbf{w}, \beta)$. This is equivalent to finding the optimal $\mathbf{w}$ that would minimize the expected square-loss $E_{\mathcal{D}}\left\{(t_n - f(x_n, \mathbf{w}))^2\right\}$. The optimal prediction is given by:

$$\begin{aligned} \mathbf{w} &= \left(\mathbf{\Phi}^T\mathbf{\Phi}\right)^{-1}\mathbf{\Phi}^T\mathbf{t} \\ and\ \mathbf{\Phi} &= \begin{pmatrix} \phi_0(x_1) & \dots & \phi_{M-1}(x_1) \\ \phi_0(x_2) & \dots & \phi_{M-1}(x_2) \\ \vdots & \ddots & \vdots \\ \phi_0(x_N) & \dots & \phi_{M-1}(x_N) \end{pmatrix} \end{aligned} \quad (3)$$

The optimal prediction for a new data point x_* is given by:

$$t_* = \mathbf{w}^T\phi(x_*) \quad (4)$$

LSR provides a closed-form solution to the regression problem. However it does not explicitly address the significance of differing amounts of data available to derive model parameters. A larger sized dataset with more training examples and stable noise parameters potentially provides more useful information for training a more accurate model than a smaller dataset. LSR is also prone to the presence of outliers because it does not take into account the consistency of points in a dataset. Another drawback of LSR is its tendency to *over-fit* to a given dataset due to which it often performs poorly on unseen data points. One solution is to include a regularization term λ that controls the relative importance of data-dependent noise. However finding the optimal λ involves techniques such as K-fold cross-validation and the need to maintain a separate validation dataset. These methods can be computationally expensive and wasteful of valuable data. A more elegant solution involves a Bayesian treatment of linear regression. Such a technique has the potential to guard against over-fitting.

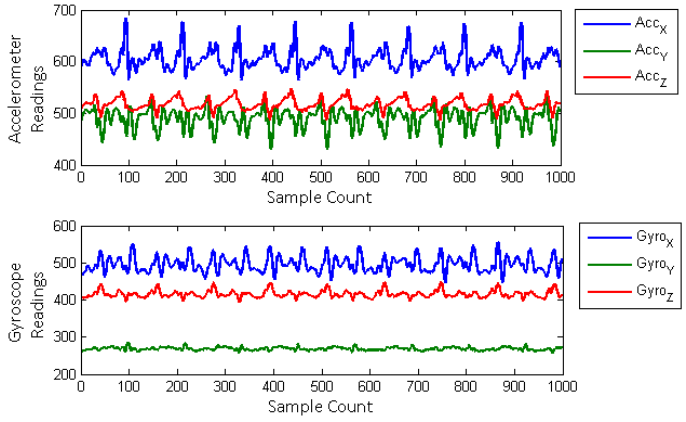

(a) An example of periodic signals obtained from the iliac crest of the right hip while walking at a constant speed of 2.5 mph. Steady state walk is cyclic in nature and this periodicity can be captured with inertial sensors.

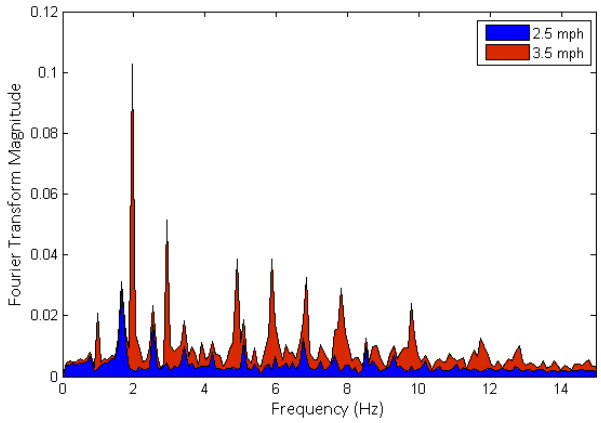

(b) Definite peaks in the Fourier transforms of the accelerometer stream on the X-axis for steady state walking at 2.5 mph and 3.5 mph suggest energy estimation by monitoring the frequency spectrum.

Figure 1: Representation of periodicity of human walk as captured by inertial sensors

C. Bayesian Linear Regression

Bayesian Linear Regression (BLR) [29] adopts a Bayesian approach to the linear regression problem by introducing a prior probability distribution over the model parameters $\mathbf{w}$ in Equation. 1. Specifically we choose a Gaussian prior over $\mathbf{w}$, $p(\mathbf{w}) = \mathcal{N}\left(\mathbf{w}; \mathbf{0}, \alpha^{-1}\mathbf{I}\right)$ where α is a hyperparameter.

Given Equation 2, the prior distribution over $\mathbf{w}$, and the properties of Gaussians, we can estimate the posterior distribution of $\mathbf{w}$ given the dataset $\mathcal{D}$ as:

$$\begin{aligned} p(\mathbf{w}|\mathbf{t}) &= \mathcal{N}(\mathbf{m}_N, \mathbf{S}_N) \\ with\ \mathbf{m}_N &= \beta \mathbf{S}_N \mathbf{\Phi}^T \mathbf{t} \\ and\ \mathbf{S}_N^{-1} &= \alpha \mathbf{I} + \beta \mathbf{\Phi}^T \mathbf{\Phi} \end{aligned}$$

The optimal prediction for a new data point is given by the predictive distribution by marginalizing over $\mathbf{w}$ as:

$$p(t_{new}|x_*, \mathbf{t}, \alpha, \beta) = \mathcal{N}(\mathbf{m}_N^T \phi(\mathbf{x}), \sigma_N^2(x_*)) \quad (5)$$

$$and\ \sigma_N^2(x_*) = \frac{1}{\beta} + \phi(x_{new})^T \mathbf{S}_N \phi(x_*) \quad (6)$$

In a fully Bayesian approach, we adopt hyperpriors over α and β also and make predictions by marginalizing over $\mathbf{w}$, α and β. However, complete marginalization over all these variables in analytically intractable. We instead adopt an iterative approach by finding the best α and β to maximize the evidence function given this dataset, find the best parameters $\hat{\mathbf{w}}$ to maximize the likelihood given a fixed α and β and repeat until convergence.

The output prediction of BLR (Equations 5 and 6) involves computing a mean $\mathbf{m}_N$ and a variance $\sigma_N^2(\mathbf{x})$. The importance of a variance estimate is that it allows the user to evaluate how "confident" the algorithm is of its prediction and provides the necessary tool to evaluate the goodness of prediction of an unseen data point. Also, it can be seen from Equation 6 that if an additional point $\mathbf{x}_{N+1}$ were added, the resultant variance $\sigma_{N+1}^2(\mathbf{x}) < \sigma_N^2(\mathbf{x})$. This tends to the limit $\sigma_N^2(\mathbf{x}) = \frac{1}{\beta}$ or the intrinsic noise in the process. Thus BLR reflects the availability of larger quantities of data through a smaller variance and hence an increasingly more confident estimate. The use of a prior α helps guard against over-fitting. α and β are derived purely from the dataset without needing a separate validation dataset.

Parametric models suffer from a shortcoming in that the form of the basis functions $\{\phi_j(\mathbf{x})\}$ are fixed before the training data set is observed. If the assumption behind the choice of basis functions or the linearity of the model is violated, the model will provide poor predictions. An alternative is to use nonparametric models where the model structure and complexity are not specified in advance but are instead determined from data.

D. Gaussian Process Regression

Given a set of training points $\{(x_1, t_1), (x_2, t_2), \ldots, (x_n, t_n)\}$ such that:

$$t_n = f(x_n) + \epsilon, \epsilon \sim \mathcal{N}\left(\mathbf{0}, \beta^{-1}\mathbf{I}\right) \quad (7)$$

a Gaussian Process Regression model (GPR) [30] estimates a posterior probability distribution over functions $f(x_1), f(x_2), \ldots f(x_N)$ evaluated at points $x_1, x_2, \ldots x_N$ such that any finite subset of the functions is a joint multivariate Gaussian distribution. Consequently, for a given set of points $x = (x_1, x_2, \ldots x_N)^T$, we have a corresponding vector $\mathcal{F}_x = (f(x_1), f(x_2), \ldots f(x_N))^T$ that belongs to a multivariate Gaussian distribution:

$$\mathcal{F}_{x_N} \sim \mathcal{N}\{\mu_N(\mathbf{x}), \mathbf{K}_N(\mathbf{x}, \mathbf{x}')\} \quad (8)$$

where $\mu(\mathbf{x})$ is the mean function $\mu(\mathbf{x}) = (\mu(x_1), \mu(x_2), \ldots \mu(x_N))^T$ and $\mathbf{K}$ is the covariance or kernel function. The key idea in GPR is that the covariance between two function values, $f(\mathbf{x}_i)$ and $f(\mathbf{x}_j)$, depends on the input values, $\mathbf{x}_i$ and $\mathbf{x}_j$ and is specified via the kernel $k(\mathbf{x}_i, \mathbf{x}_j)$. The kernel function returns the covariance between the corresponding $\mathcal{F}_x$ variables $f(\mathbf{x}_i)$ and $f(\mathbf{x}_j)$. To completely specify a GP, it is enough to specify $\mu(\mathbf{x})$ and $\mathbf{K}(\mathbf{x}, \mathbf{x}')$. By definition, each $f(\mathbf{x}_i)$ is marginally Gaussian, with mean $\mu(\mathbf{x}_i)$ and variance $k(\mathbf{x}_i, \mathbf{x}_i)$.

Typically, for ease of implementation, the mean of the dataset is subtracted from each data point so that the mean function is $\mathbf{0}$. To reflect that similar feature vectors with small interpoint Euclidean distance are more likely to correspond to the same output energy consumption measure, and to capture the inherent common structure represented by feature vectors due to an underlying periodicity in walking, we choose the radial basis function kernel. Further, to capture the fact that we only have access to noisy observations of the function values, it is necessary to add the corresponding covariance function

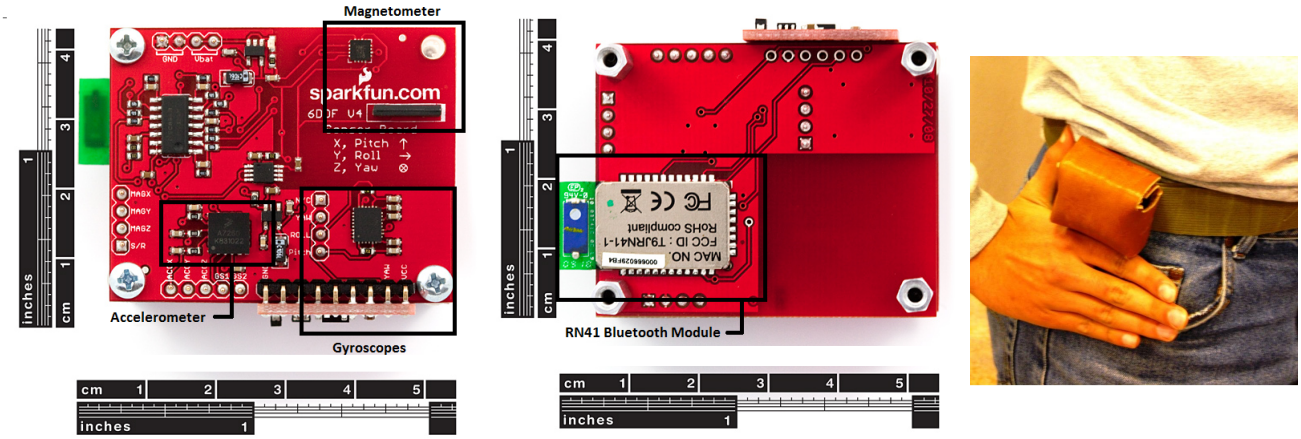

(a) Sensor board used to collect data.

(b) The controller board with RN-41 Bluetooth module

(c) An example mount of sensor on the right iliac crest.

Figure 2: Illustration of hardware used to capture treadmill walking information. Acceleration information was collected with a Freescale MMA7260Q triple-axis accelerometer. Rotational rates were collected with 2 Invensense IDG500 500°/s gyroscopes mounted perpendicular to each other. The sensor hardware was modified to be worn with a custom designed harness on the right iliac crest. Original image source for (a) and (b): www.sparkfun.com

for noisy observations. The complete kernel function can be expressed in element by element fashion as:

$$k(x_i, x_j) = \sigma_f^2 . e^{-\frac{1}{2l^2}|x_i - x_j|^2} + \sigma_n^2 \delta_{ij} \quad (9)$$

where σ_f^2 is the signal variance, l is a length scale that determines strength of correlation between points, σ_n^2 is the noise variance.

For a new point x_* there exists a corresponding target quantity $f(x_*)$. Since $f(x_*)$ also belongs to the same GP, it can be appended to the original training set to obtain a larger set.

$$\mathcal{F}_{x_{N+1}} \sim \mathcal{N}\{\mu_N(\mathbf{x}), \mathbf{K}_{N+1}(\mathbf{x}, \mathbf{x}')\} \quad (10)$$

$$K_{N+1} = \begin{pmatrix} \mathbf{K}_N & \mathbf{k}_* \\ \mathbf{k}_*^T & k \end{pmatrix} \quad (11)$$

where $\mathbf{k}_*$ has elements $k(x_n, x_*)$ for $n = 1, \ldots, N$ and $k(x_i, x_j)$ is defined in Equation 9. Using properties of Gaussians and the definition of GPs, it follows that for a new test point $p(t_*|x_*, \mathbf{X}, \mathbf{t}) = \mathcal{N}(f(x_*); m(x_*), \sigma_{x_*}^2)$. Because this joint distribution is Gaussian by definition, we have:

$$m(x_*) = \mathbf{k}_*^T \mathbf{K}_N^{-1} \mathbf{t} \quad (12)$$

$$\sigma^2(x_*) = k - \mathbf{k}_*^T K_N^{-1} \mathbf{k}_* \quad (13)$$

Thus estimating a target energy from training data amounts to evaluating $\mathbf{K}_N$, $\mathbf{k}$ and c and using values shown in Equations. 12 and 13.

Equations. 12 and 13 summarize the key advantages of GPR. Again, the use of a probabilistic model to obtain a mean and variance for each prediction allows the user to assess the confidence of each prediction. In contrast to BLR however, GPR is non-parametric: its model complexity increases with larger quantities of data as evident from the increasing size of the kernel matrix. GPR avoids the process of explicitly constructing a suitable feature function space by dealing instead with kernel functions. As the kernel implicitly contains a non-linear transformation, no assumptions about the functional form of the feature space are necessary. This allows us to deal with non-linear maps without having to construct non-linear function spaces. The motivation behind considering this algorithm was to determine whether using a nonlinear probabilistic map (GPR) offers benefits over a linear probabilistic map (BLR) in terms of increased prediction accuracy.

V. Methods

A. Hardware Description

Human movement was captured with a modified version of the Sparkfun 6DoF Inertial Measurement Unit (IMU) v4 [31]. Fig. 2 illustrates the hardware used. The v4 provides three axes of acceleration data, three axes of gyroscopic data, and three axes of magnetic data with three sensors: a Freescale MMA7260Q triple-axis accelerometer, set at 1.5 g sensitivity and two InvenSense IDG500 500°/s gyroscopes. At the time of this study, the absence of triaxial gyroscopes required that two biaxial gyroscopes be mounted perpendicular to each other and calibrated to function as one gyroscope. Control was through an LPC2138 ARM7 processor. Custom firmware was used on the controller board to stream sensor data continuously. Data were sampled at 100 Hz. The unit used Bluetooth to transmit data to either a nearby PC or mobile phone using the RN41 Bluetooth module set at 115200 bps. Maximum range of the transmitter was approximately 5 m in indoor conditions. The system was powered from a 3.3V rechargeable lithium-polymer battery power supply. The sensor was encased in a custom-designed harness to be worn on the right iliac crest (participants were asked to wear the harness tightly to prevent any slippage). The use of sensors in all three axes allowed the capture of periodicity in all three planes – sagittal, frontal and transverse. The treadmill used for the experiments was the research quality NordicTrack A2550 PRO. Fig. 7a illustrates the recording procedure [6].

B. Participant Statistics

Seven healthy adults (three male, four female) participated in the study. Height and weight of each participant were recorded using a Healthometer balance beam scale. The participants had average age = 29 ± 6 years, average height =

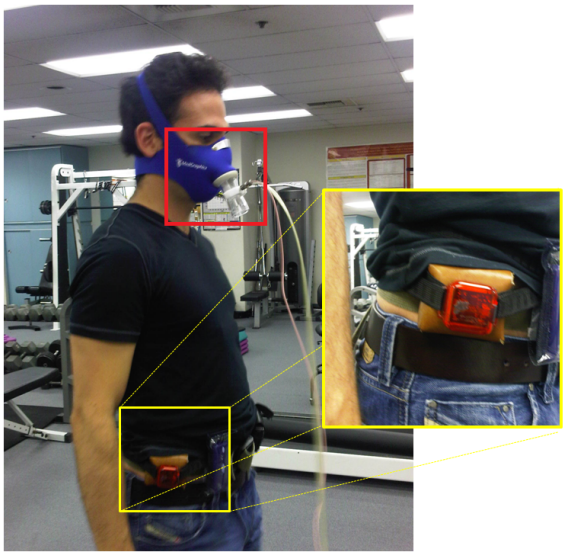

Figure 3: An example recording procedure for a single participant. The yellow box indicates sensor mounting. The red box indicates VO_2 recording via the mask leading to the metabolic cart.

1.67 ± 0.10 m, average weight = 66 ± 17 kg and average BMI = 24 ± 8. Informed written consent was obtained from participants and the study was approved by the Institutional Review Board at the University of Southern California. Participants walked at 11 predetermined speeds between 2.5 mph and 3.5 mph in intervals of 0.1 mph. Speeds were chosen based on the Compendium of Physical Activities [32]. Rate of oxygen consumption ($\dot{V}O_2$, mL/min) was used as the representation of energy expenditure. This was measured using the MedGraphics Cardio II metabolic system with BreezeSuite v6.1B (Medical Graphics Corporation). The metabolic system outputs data at the frequency of every breath. Before each test, the flow meter was calibrated against a 3.0 L syringe and the system was calibrated against O_2 and CO_2 gases of known concentration. The duration of walking data collected for each speed was 7 minutes with two minutes of changeover time to allow for settling of $\dot{V}O_2$ consumption. For each participant, data were recorded in two sessions with the first session consisting of speeds 2.5 mph, 2.8 mph, 3 mph, 3.3 mph and 3.5 mph and the second session at the remaining speeds.

C. Data Collection and Pre-processing

Each sensor stream from the IMU was passed through a lowpass filter with 3dB cutoff at 20 Hz. This frequency was chosen keeping in mind that everyday activities fall in the frequency range of 0.1-10 Hz [33]. Each stream was divided into 10 second epochs. Within each epoch, the 1024 point normalized FFT was extracted to obtain frequency information. The $\dot{V}O_2$ values from the MedGraphics metabolic system that fell within each epoch were averaged and matched appropriately. The 10 second interval was chosen based on previous successful implementations [6] on this time scale. Each 10 second $FFT - \dot{V}O_2$ pair consists of one data point. Thus for each participant's complete recording session, the dataset consists of approximately 77 minutes of data (or 460 data points). Thus data for each user consisted of a sequence of epochs, each containing features from the IMU and the average rate of oxygen consumption ($\dot{V}O_2$) for that epoch.

D. Training and Testing Procedure

In each participant's data, we assume that each $FFT - \dot{V}O_2$ pair is independent and identically distributed (i.i.d). Thus one can treat each point as independent from any other in the dataset given the model. This need not necessarily hold for general walking but follows from our steady-state assumption in treadmill walking. A fraction of the data were uniformly sampled and partitioned into training data, the remaining fraction constituting test data. Different models were trained with the same training data but with different feature vectors and candidate algorithms. RMS error was calculated as a measure of accuracy. This was repeated over 10 trials for different randomly sampled data and results averaged. This was repeated for training data percentages from 10% to 90% and constituted a per-subject measure of performance. The results were then averaged over all subjects. To understand the context behind the relative magnitude of the errors, it must be noted that the $\dot{V}O_2$ values were in the range of 400-1000 mL/min.

VI. Results and Discussion

This section provides a comparative analysis of prediction accuracy based on different models. We varied the models along three dimensions. First, we considered the effect of different sensor streams. Our study used two kinds of inertial sensors: triaxial accelerometers and triaxial gyroscopes. Within data from each inertial sensor, we compared the effect of using triaxial information versus uniaxial information. Using the best feature space from each of these comparisons, we compared the utility of accelerometers, gyroscopes and a combined solution using both sensors in terms of prediction accuracy. Second, using the best feature space from the first study, we compared the relative performance of algorithms measured by prediction accuracy. Finally, we performed an empirical comparison of algorithm run time to provide further insight into algorithm choice based on the trade-off between prediction accuracy and computational capability. The motivation behind comparing these models was to understand the issues related to optimal representation of treadmill walking to predict energy consumption given a set of inertial sensors. Unless otherwise stated, results were significant ($p < 0.05$ on a per-subject basis).

A. Comparison across Feature Spaces

1) Single sensor feature space comparison: Fig. 4 groups results accordingly. Each panel consists of testing errors when single axes features are used with a fourth series consisting of triaxial features. Results are grouped columnwise by sensor type (accelerometer or gyroscope) and row-wise by algorithm type (LSR, BLR and GPR).

LSR was sensitive to the quantity of training data available regardless of the sensor. Error using single axis streams peaked when 30% of the training data were used. This was not true when triaxial features were used. At lower percentages of training data, the presence of noisy data points biases predictions. As more data are available, the biasing effect of noisy data points is reduced. The use of triaxial features avoids this with a higher dimensional feature space. However as more training data are available, the model based on triaxial features begins to over-fit to the dataset. BLR and GPR are less prone to over-fitting at all percentages. With BLR and GPR, increasing the percentage of training data reduced prediction errors for

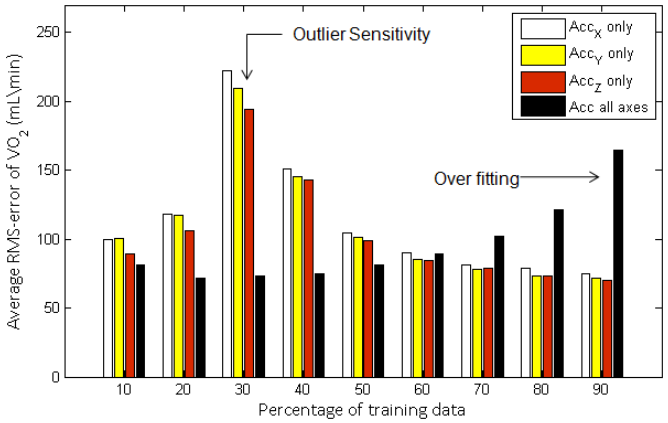

(a) LSR with accelerometer features only.

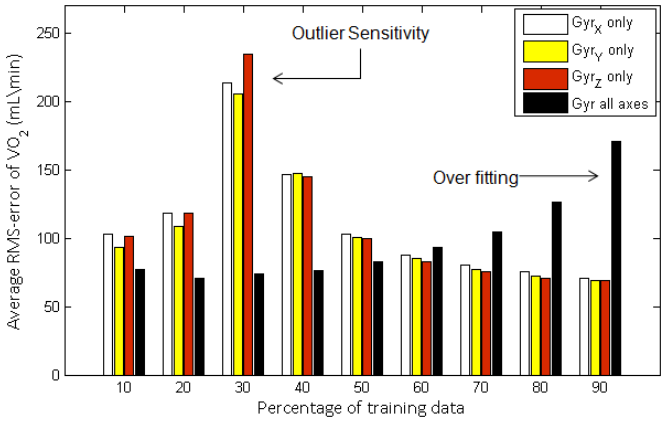

(b) LSR with gyroscope features only

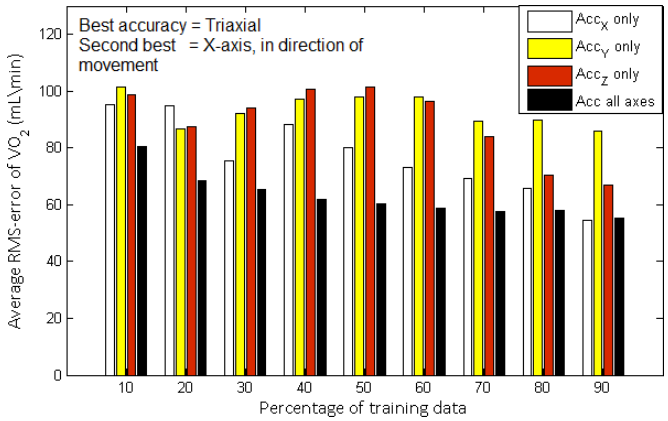

(c) BLR with accelerometer features only

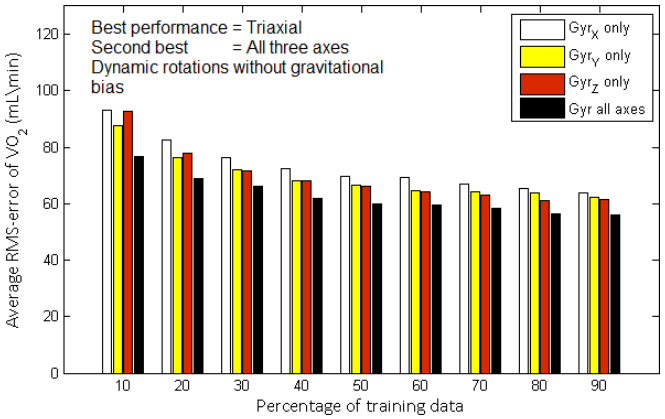

(d) BLR with gyroscope features only

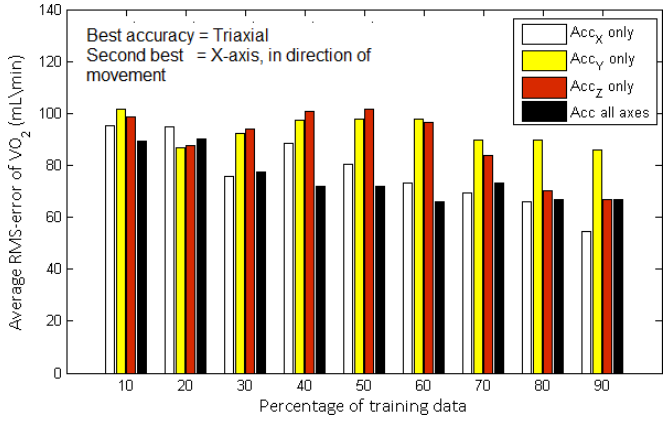

(e) GPR with accelerometer features only

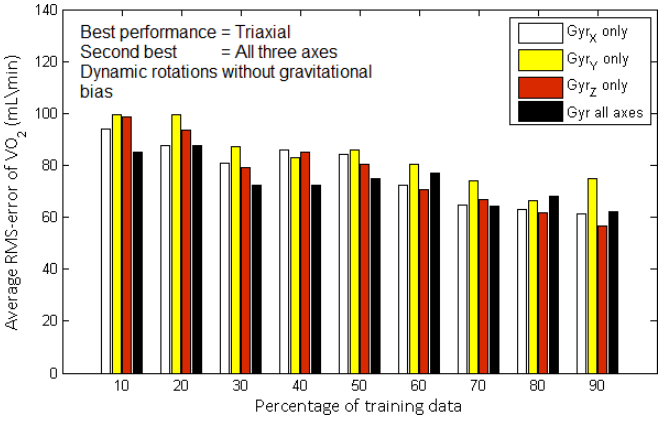

(f) GPR with gyroscope features only

Figure 4: Illustration of variation of prediction accuracy (measured by Average RMS prediction error across all participants) with different combinations of feature vectors. Results are grouped row-wise by algorithm and column wise by sensor stream. LSR results depended heavily on the number of points used due to over-fitting and presence of outliers. BLR and GPR showed consistently reduced errors with increase in training data size. In the case of BLR and GPR, use of all 3 axes as features improved prediction accuracy as opposed to using just one sensor axis. Among accelerometer features using X-axis acceleration alone showed the next lowest prediction error. This is most likely because the X-axis was aligned with the direction of forward movement. All three gyroscopic axes showed comparable errors. Gyroscope features in Y and Z axes showed lower errors than corresponding acceleration Y and Z axes. This was most likely due to gyroscopes only capturing dynamic movement free from gravitational bias. Gyroscopes were capable of providing equivalent if not better results for energy prediction from treadmill walking.

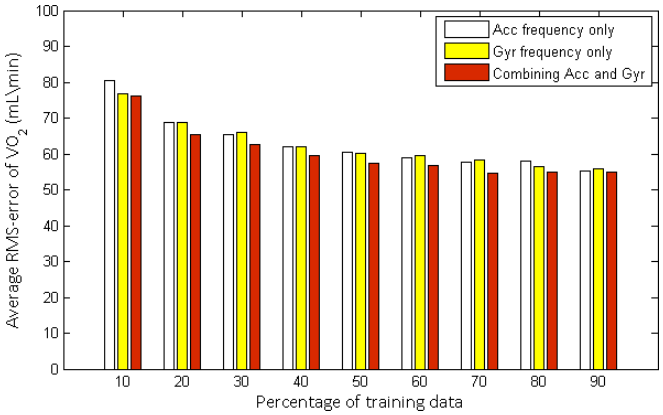

(a) In the case of BLR, accelerometer and gyroscopic information show similar prediction accuracies. Combining accelerometer and gyroscopic information shows lower prediction errors.

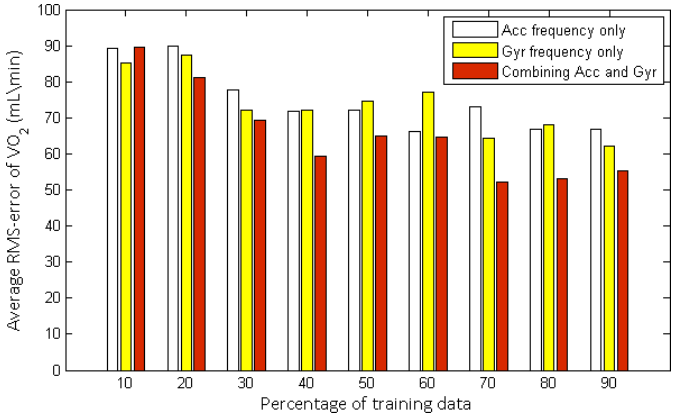

(b) In the case of GPR, combining accelerometer and gyroscopic information shows lower prediction errors. The decrease in error is higher than in the case of BLR because GPR predicts information based on covariances between data points and hence incorporates relationships between similar data points as well.

Figure 5: Illustrating the effect of combining triaxial accelerometer and gyroscopic information (measured by average RMS prediction error across all participants) in the case of BLR and GPR. Accelerometer and gyroscope provide similar results when used separately.

that space. For these reasons, in the remainder of this paper, we focus on results obtained from BLR and GPR.

With accelerometer information alone, the errors in increasing order were: triaxial accelerations, X-axis accelerations, Z-axis accelerations and Y-axis accelerations. Using all three axes had the effect of introducing redundancy, resulting in better prediction accuracies. The second best error can be understood by the fact that the dominant acceleration when wearing the sensor in the right hip is in the up-down direction of movement. Movement in this plane represents the best single-axis indicator for predicting energy expenditure. Triaxial information improved prediction. The reduction in error when only Y-axis features were used was comparatively less. Y axis features represent movement in the forward-backward direction. Thus, this could be because of the natural tendency of participants to speed up or down slightly (this constitutes an acceleration or deceleration) while walking to maintain constant position on the treadmill. This would result in a noisy feature vector in this direction.

With gyroscopic information alone, all individual axes showed similar errors. Triaxial information yielded higher accuracy. Gyroscopes track rotational rates of the human body rather than accelerations. Hence they are less prone to acceleration in a particular direction. Gyroscopes are also more tolerant to minor changes in position of mounting. Also, gyroscopes capture only dynamic movement free from gravitational bias. All these factors contributed to consistent prediction across all three axes when gyroscopes were used. Finally, the range of errors obtained when only gyroscopes are used was comparable and in some cases even better than that when only accelerometers were used. This suggests the feasibility in using gyroscopes to track dynamic activities either as a separate sensor or in combination with accelerometers.

2) Comparison between accelerometer and gyroscopic data: Fig. 5 outlines the results when BLR and GPR-based models are used. In both cases, using only gyroscope data provided comparable average RMS errors to using only accelerometer data. Additionally, combining accelerometer and gyroscope information reduces prediction errors. The error reduction obtained from combining sensor information was

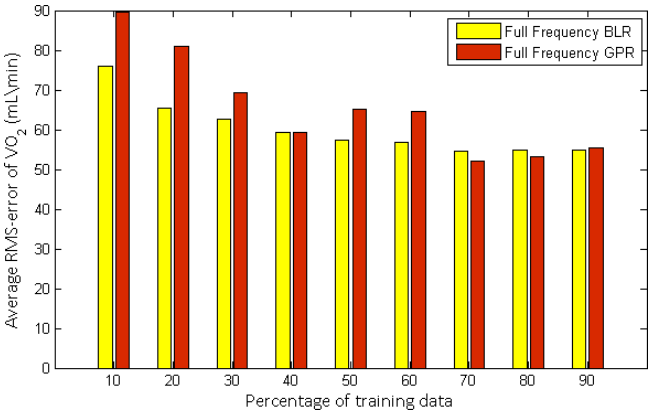

Figure 6: Illustration of relative algorithmic performance when triaxial information from all sensors is used (measured by average RMS prediction error across all participants). With increasing number of data points GPR begins to perform comparably with BLR.

more pronounced in the case of GPR than LSR. This can be understood from the fact that GPR based models are based on covariances or similarities between data points rather than an explicit dependence on features (Section IV-D). Additional information by way of gyroscopes provides further evidence that a certain data point belongs to a particular class. This enhanced the modeling capability of GPR. By contrast, BLR is based on obtaining weights for features from training. For the same "kind" of walking the periodicities exhibited would remain the same for both accelerometers and gyroscopes. Thus addition of gyroscopic features simply amounts to a redistribution of the original weights from single sensor data to both sensor streams.

B. Comparison across Algorithms

1) Algorithm accuracy: Fig. 6 illustrates the results obtained from comparing a nonlinear approach (GPR) with a linear approach (BLR). Both GPR and BLR performed better when more training data are used. With increasing training

data, GPR performance improved gradually until it was comparable with BLR. Nonlinear approaches require more data to be able to capture nonlinear subtleties and prevent over-fitting to noise. When data from each subject were considered, GPR showed a lower average RMS prediction error when compared with BLR and LSR when a larger relative percentage of training data was used. This indicates that GPR shows superior performance when a large quantity of data are available. With smaller quantities of data it would be advisable to use BLR to prevent over-fitting.

Fig. 7a illustrates an example output for energy prediction for a single participant using the feature space and algorithm combination that provides the lowest prediction error. The model uses triaxial features from both accelerometer and gyroscope axes and GPR with 80% of the data used for training. The predicted values (shown in blue) closely match the ground truth (shown in red). Fig. 7b shows the same data as a scatter plot with ground truth displayed on the X-axis and GPR predicted values on the Y-axis. The two times series showed an average correlation of 0.92 across users.

C. Algorithm Run Time

Parametric approaches like linear regression depend on the dimension of the input data space, d and learning is of order $O(d^3)$. Nonparametric approaches depend on the number of data points. In particular, for N data points, GPR requires the inversion of an $N \times N$ matrix which is an $O(N^3)$ operation. Knowing the run time for training is important to understand the tradeoffs between prediction accuracy and time of training. This is particularly important if these algorithms are to be implemented in resource-constrained platforms such as mobile phones or portable PCs. In our study, there were three classes of data types: Single sensor (either accelerometer or gyroscope) with only one axis in use, single sensor with all three axes in use and both sensors all three axes in use. Each of these cases multiplies the feature space used by 3. In addition, three algorithms: LSR, BLR and GPR were used. Fig. 8 illustrates our results for one participant. Similar trends exist for all participants.

For this study, the time taken to train a dataset with different percentages of training data for one participant was recorded in the case of one feature space and one algorithm. Prediction accuracies were also measured. A scatter plot was created with prediction accuracies on the X-axis and algorithm run time on the Y-axis (Log-scale, base 10) with all training percentages represented as one class. This was repeated for different combinations of feature vectors and algorithms. In all plots, feature spaces are coded by color (Blue: single sensor, single axis; Red: single sensor, all axes; Green: both sensors, all axes) and algorithms are coded by symbol (LSR: empty square; BLR: filled circle; GPR: empty star). For clarity, plots are shown in two views.

Fig. 8a shows a comparative analysis of run time versus accuracy for BLR and LSR. In the case of LSR, addition of extra features showed no benefits in terms of accuracy but increases run time. Addition of features improved BLR prediction accuracy at the expense of higher run time. However in our study, the absolute run time for training was still on the order of a few seconds and less than 30 seconds in all cases for all participants. The consistency of results and lower error rates along with reasonable training run times justifies the selection of BLR over LSR with any combination of feature vectors. Using both sensors offers limited advantage in terms of prediction accuracy but requires larger run times. Therefore, it would be advisable in resource-constrained systems to choose a model that only uses one of either sensor for training if accuracy is not an issue.

Fig. 8b shows a comparative analysis of run time versus accuracy for BLR and GPR. Both BLR and GPR are probabilistic approaches and hence show consistently better results with increasing dataset size. Nonlinear modeling with GPR showed lower or comparable errors as BLR, particularly when more training data were used. However, the run time was at least two orders of magnitude higher. To provide intuition behind such run time, we observe that a $\dot{V}O_2$ estimation error of 35 mL/min (best accuracy possible in our study with BLR for this participant) corresponds roughly to a percentage error of 5% or lower. To go from 35 mL/min to 30 mL/min (best accuracy possible with GPR for this participants) corresponds to obtaining a percentage error of 4% or lower. Given a dataset, to be able to obtain a higher accuracy requires increasingly larger computing power to accommodate more sophisticated models. In resource-constrained systems, this incremental increase in accuracy might not be justified. Therefore if computing power is an issue, it would be advisable to use linear models over nonlinear models.

D. Accounting for Reciprocal Limb Movement

A limitation of our approach is that we neglect the energy cost for reciprocal limb movement. Robertson and Winter [34] showed that the energy transfer among limb segments can be both complex and significant. Neglecting this energy transfer can lead to a source of inaccuracy in energy estimation. Cavagna et al. [35] used a simple pendulum model to account for the differences in energy transfer during walking. Their study reported that the model is valid for a narrow range of speeds ($\approx$ 4 km/hr). At these speeds the work done to lift the center of mass of the body (W_v) is equal to the total mechanical energy (W_t) expended. This model deviates from the ideal simple pendulum case (at lower speeds $W_t < W_v$ and at higher speeds $W_t > W_v$).While our current suite of sensors does not allow the tracking of joint energy transfer, the above studies indicate that the speed of walking can be used to track the variations. While in more practical implementations such as portable energy estimation of walking, measuring speed directly might not be possible, in future laboratory work we plan to measure the the effect of neglecting speed for both treadmill and overground walking. Another technique is to maintain a complete user state in the form of a Bayesian network, with each node corresponding to a particular limb state. Monitoring limb states indirectly can also potentially lead to improved models. This however requires the placement of additional sensors on limbs. We plan to pursue this as part of a long term effort to both quantify how much error is caused by neglecting such parameters and to improve prediction accuracy.

VII. Conclusion And Future Work

Walking is one of the easiest and commonly available activities to maintain an active lifestyle. Being able to accurately characterize intensity of walking represents an important step in public health delivery because it allows development of appropriate interventions based on objective measures. Existing accelerometer-based commercial activity monitors rely on "counts" to represent activity information. This does not have

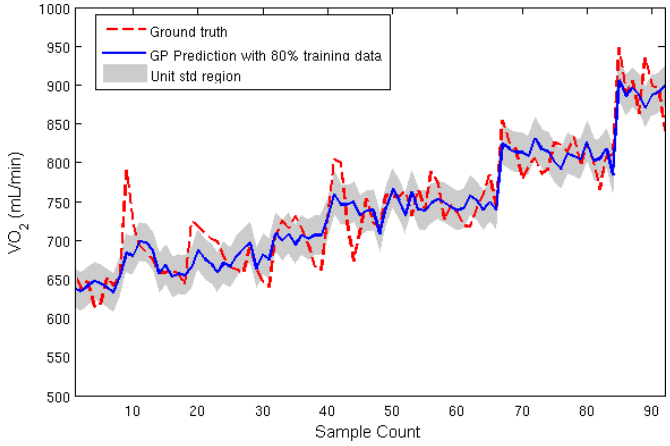

(a) An example prediction for a randomly selected test dataset from a single subject. Sample number is on the X-axis. The ground truth is displayed in red and output from GPR in blue with associated prediction variance in gray. Predicted values closely match the ground truth.

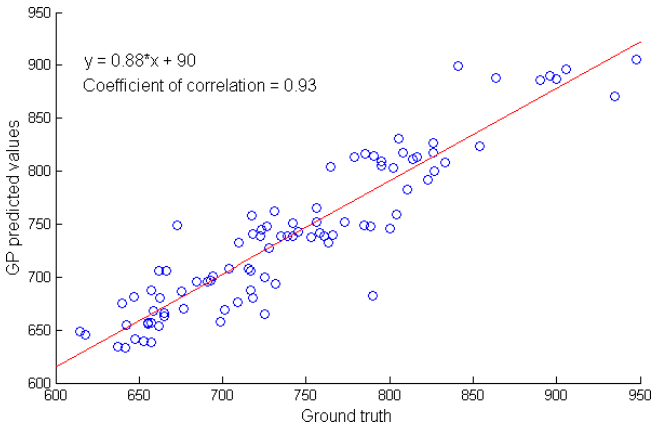

(b) An example scatter plot showing GPR prediction versus ground truth obtained for a single participant. Predicted points showed a high positive correlation of 0.92 across subjects.

Figure 7: An example prediction using the algorithm and feature combination that provided the least error across subjects using all sensor streams and all axes with Gaussian Process Regression (GPR) as the training algorithm.

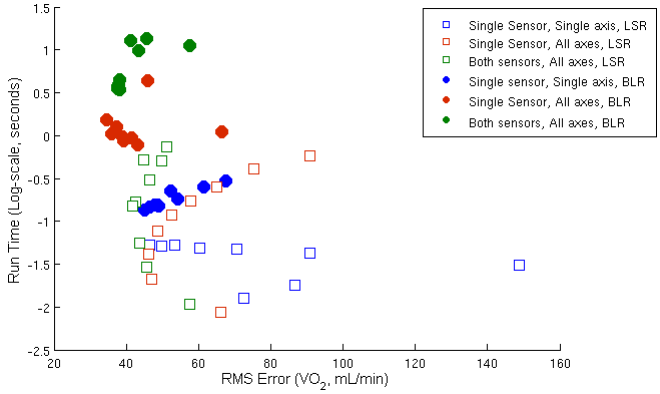

(a) Scatter plot comparing the relationship between run time and prediction accuracy for BLR (filled circles) and LSR (squares) when different features are used. Run time is shown in a logarithmic scale. BLR shows lower errors but has a higher run time. In the case of LSR, addition of extra features shows no apparent benefits in terms of accuracy but increases run time. Addition of features improves BLR prediction accuracy measured by consistency of prediction and error rate at the expense of higher run time. However absolute run time is still on the order of a few seconds which justifies the selection of BLR over LSR.

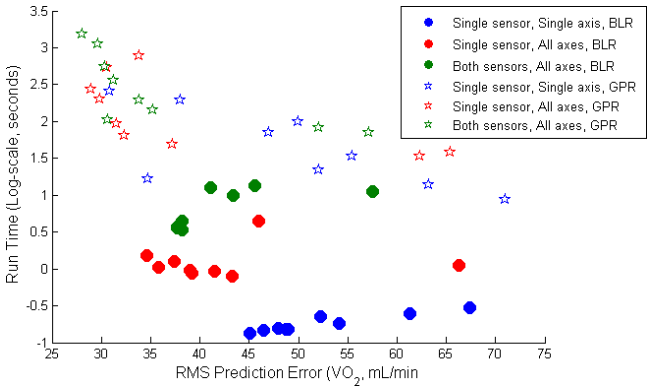

(b) Scatter plot comparing the relationship between run time and prediction accuracy for BLR (filled circles) and GPR (stars) when different features are used. Run time is shown in a logarithmic scale. Nonlinear modeling with GPR shows lower errors than BLR, particularly when more training data are used. However, the run time is at least two or three orders of magnitude higher. This shows that for the same dataset, increasingly higher accuracy requires much more computing power. This represents an important trade-off between the level of accuracy desired and the algorithm to choose.

Figure 8: An illustration of the relationship between accuracy and run time for LSR, BLR and GPR for a single participant. Scatter points of each class represent different training percentages of the same class and feature space. The best algorithm has to be as close to the origin as possible (lowest error and lowest run time)

a physically intepretable meaning. Also, current monitors do not yet incorporate gyroscopic measurements to characterize movement. Being able to accurately represent human activity and derive physiological measures such as energy expenditure requires that one extracts meaningful and complete properties of human movement from raw data and develop relevant maps from these properties.

In this paper, we described an experimental study to estimate energy expenditure during treadmill walking using a single hip-mounted inertial sensor comprised of a triaxial accelerometer and a triaxial gyroscope. Our approach involved representing the cyclic nature of walking using Fourier transforms of triaxial accelerometer and gyroscopic sensor streams and establishing a relationship between Fourier domain features and energy expended. We described three regression techniques: Least Squares Regression (LSR), Bayesian Linear Regression (BLR) and Gaussian Process Regression (GPR) and showed their applicability to this problem.

We report and compare prediction accuracies using different sensor streams and algorithms. LSR results depended heavily on the number of points used for training. This was because LSR is prone to over-fitting and the presence of outliers. BLR and GPR showed consistently reduced errors with increasing training data size. While employing BLR, accelerometer and gyroscope data simultaneously improved prediction accuracy. Among accelerometer features, X-axis acceleration showed the lowest prediction error. This was because the X-axis was aligned with the direction of forward movement. All three gyroscopic axes showed comparable errors. Using gyroscope features in Y and Z axes showed lower errors than correspond-

ing acceleration Y and Z axes. This is most likely due to gyroscopes only capturing dynamic rotational movement free from gravitational bias. Gyroscopes were capable of providing equivalent if not better results for energy prediction from treadmill walking. Additionally, combining accelerometer and gyroscope information reduced prediction errors. With increasing training data, GPR performance improved till it was comparable to BLR highlighting the need for more data for nonlinear approaches. However, GPR training time was at least two orders of magnitude higher. Therefore if computing power is an issue, it would be advisable to use linear models like BLR over nonlinear models and trading off accuracy.

We plan to expand our work in a number of directions. We are currently working on developing generalized models that are applicable across a range of physiological parameters such as height, weight, BMI, gender and age. This involves undertaking a larger study and collecting movement information for treadmill walking. We are developing a generalized linear model similar to Bayesian Linear Regression with informative initial conditions based on physiological parameters.

Another important issue is that we restrict ourselves to steady-state walking on a level plane. While our results are promising, further work is needed to generalize to overground walking in free-living conditions. For this we plan to study the performance of our algorithms for overground walking. If successful, this has the potential to vastly benefit the field of human calorimetry by providing accurate $\dot{V}O_2$ values while offering the convenience and cost-effectiveness of inertial sensor based activity monitoring. We also plan to undertake similar analyzes for other kinds of cyclic activities still operating under the steady-state condition. In doing so, we plan to explore whether our methods can be applied in the more general framework of energy expenditure for repetitive activities.

VIII. Acknowledgments

The authors would like to thank David Erceg of the Division of Biokinesiology and Physical Therapy, USC, for his invaluable support and guidance.

The authors would also like to thank the reviewers and editors for their valuable suggestions and comments.

References

[1] "World Health Organization - Physical Activity." http://www.who.int/dietphysicalactivity/pa/en/index.html, January 2010.

[2] D. E. Warburton, C. Whitney, and S. S. Bredin, "Health Benefits of Physical Activity," *CMAJ*, vol. 174, 2006.

[3] K. Aminian and B. Najafi, "Capturing human motion using body-fixed sensors: outdoor measurement and clinical applications," *Computer Animation and Virtual Worlds*, vol. 15, no. 2, pp. 79–94, 2004.

[4] G. Meijer, K. Westerterp, F. Verhoeven, H. Koper, and F. ten Hoor, "Methods to assess physical activity with special reference to motion sensors and accelerometers," *Biomedical Engineering, IEEE Transactions on*, vol. 38, pp. 221–229, March 1991.

[5] A. L. Dunn, B. H. Marcus, J. B. Kampert, M. E. Garcia, H. W. Kohl III, and S. N. Blair, "Comparison of Lifestyle and Structured Interventions to Increase Physical Activity and Cardiorespiratory Fitness: A Randomized Trial," *JAMA*, vol. 281, no. 4, pp. 327–334, 1999.

[6] H. Vathsangam, A. Emken, D. Spruijt-Metz, T. E. Schroeder, and G. S. Sukhatme, "Energy Estimation of Treadmill Walking using On-body Accelerometers and Gyroscopes," in *32nd Annual International Conference of the IEEE Engineering in Medicine and Biology Society*, 2010.

[7] C. Bouten, K. Westerterp, M. Verduin, and J. Janssen, "Assessment of energy expenditure for physical activity using a triaxial accelerometer.," *Med Sci Sports Exercise*, vol. 26, no. 12, pp. 1516–1523, 1994.

[8] M. J. Mathie, A. C. Coster, N. H. Lovell, and B. G. Celler, "Accelerometry: providing an integrated, practical method for long-term, ambulatory monitoring of human movement.," *Physiological measurement*, vol. 25, April 2004.

[9] S. E. Crouter, K. G. Clowers, and D. R. Bassett, "A novel method for using accelerometer data to predict energy expenditure.," *J Appl Physiol*, vol. 100, pp. 1324–1331, Apr 2006.

[10] P. S. Freedson, E. Melanson, and J. Sirard, "Calibration of the computer science and applications, inc. accelerometer.," *Medicine and science in sports and exercise*, vol. 30, pp. 777–781, May 1998.

[11] N. Klippel and D. Heil, "Validation of energy expenditure prediction algorithms in adults using the actical electronic activity monitor," *Med Sci Sports Exerc*, vol. 35, 2003.

[12] J. J. Reilly, L. A. Kelly, C. Montgomery, D. M. Jackson, C. Slater, S. Grant, and J. Y. Paton, "Validation of actigraph accelerometer estimates of total energy expenditure in young children.," *Int J Pediatr Obes*, vol. 1, no. 3, pp. 161–167, 2006.

[13] G. Plasqui and K. R. Westerterp, "Physical activity assessment with accelerometers: An evaluation against doubly labeled water," *Obesity*, vol. 15, pp. 2371–2379, Oct. 2007.

[14] R. P. Troiano, "Translating accelerometer counts into energy expenditure: advancing the quest.," *J Appl Physiol*, vol. 100, pp. 1107–1108, 2006.

[15] D. P. Heil, "Predicting Activity Energy Expenditure Using the Actical Activity Monitor," *Research Quarterly for Exercise and Sport*, vol. 77, p. 64, March 2006.

[16] A. Godfrey, R. Conway, D. Meagher, and G. Laighin, "Direct measurement of human movement by accelerometry," *Medical Engg. & Phy.*, vol. 30, pp. 1364–1386, 2008.

[17] M. Tapia, *Using machine learning for real-time activity recognition and estimation of energy expenditure*. PhD thesis, Massachusetts Institute of Technology. Dept. of Architecture. Program in Media Arts and Sciences., 2008.

[18] M. Rothney, M. Neumann, A. Beziat, and K. Chen, "An artificial neural network model of energy expenditure using nonintegrated acceleration signals," *J Appl Physiol*, vol. 103, pp. 1419–27, October 2007.

[19] F. Albinali, S. Intille, W. Haskell, and M. Rosenberger, "Using wearable activity type detection to improve physical activity energy expenditure estimation," in *12th conference on Ubiquitous Computing*, 2010.

[20] A. V. Rowlands, "Accelerometer assessment of physical activity in children: an update.," *Pediatr Exerc Sci*, vol. 19, pp. 252–266, Aug 2007.

[21] J.-C. Cheng and J. M. F. Moura, "Tracking human walking in dynamic scenes," in *ICIP '97: Proceedings of the 1997 International Conference on Image Processing (ICIP '97) 3-Volume Set-Volume 1*, (Washington, DC, USA), p. 137, IEEE Computer Society, 1997.

[22] B. Zappa, G. Legnani, A. J. van den Bogert, and R. Adamini, "On the number and placement of accelerometers for angular velocity and acceleration determination," 2001.

[23] "Single-chip triaxial gyro from invensense." http://www.sensorsmag.com/product/single-chip-triaxial-gyro-invensense, 2009.

[24] C. Chang, R. Ansari, and A. Khokhar, "Efficient tracking of cyclic human motion by component motion," no. 12, pp. 941–944, 2004.

[25] *ACSM's Guidelines for Exercise Testing and Prescription*. American College of Sports Medicine, 2010.

[26] V. Bunc and R. Dlouha, "Energy cost of treadmill walking," 1997. Anglais.

[27] M. Pearce, D. Cunningham, A. Donner, P. Rechnitzer, G. Fullerton, and J. Howard, "Energy cost of treadmill and floor walking at self-selected paces," *European Journal of Applied Physiology and Occupational Physiology*, vol. 52, pp. 115–119, 1983. 10.1007/BF00429037.

[28] C. M. Bishop, *Pattern Recognition and Machine Learning (Information Science and Statistics*. Springer-Verlag, 2006.

[29] A. Gelman, J. B. Carlin, H. S. Stern, and D. B. Rubin, *Bayesian Data Analysis, Second Edition*. Chapman and Hall/CRC, 2 ed., July 2003.

[30] C. K. I. Williams, "Prediction With Gaussian Processes: From Linear Regression To Linear Prediction And Beyond," pp. 599–621, 1997.

[31] Sparkfun, "6 Dof v4 Datasheet - http://www.sparkfun.com/datasheets/Sensors/IMU/6DOF-v4-Rev1.pdf," 2009.

[32] B. Ainsworth, W. Haskell, M. Whitt, M. Irwin, A. Swartz, S. S. W. O'Brien, D. B. Jr, K. Schmitz, P. Emplaincourt, D. J. Jr, and A. Leon, "Compendium of physical activities: An update of activity codes and met intensities.," *Med Sci Sports Exerc*, vol. 32, pp. S498–S516, 2000.

[33] L. Bao and S. S. Intille, "Activity recognition from user-annotated acceleration data," April 2004.

[34] R. DG and W. DA, "Mechanical energy generation, absorption and transfer amongst segments during walking," *J Biomech.*, vol. 13, pp. 845–54, 1980.

[35] G. Cavagna, H. Thys, and A. Zamboni, "The sources of external work in level walking and running.," *J. of Physiology*, vol. 262, pp. 639–657, 1976.

Harshvardhan Vathsangam received the B. Tech. degree in Engineering Physics from the Indian Institute of Technology Madras, Chennai, India in 2008. He is currently a PhD student with the Robotic Embedded Systems Laboratory, Viterbi School of Engineering, University of Southern California, Los Angeles, CA. He is a recipient of the Annenberg Graduate Fellowship. His research interests are in the application of statistical machine learning techniques for inertial data from the human body for physical activity detection and energy expenditure monitoring.

B. Adar Emken received the B.S. in Behavioral Neuroscience from Ohio State University, Dublin, OH in 2001 and the Ph.D. in Neurosience from University of California, Irvine in 2008.
She joined the Department of Health Promotion and Disease Prevention, University of Southern California, Los Angeles, CA, in 2008 as a Postdoctoral fellow, to design a wireless body area network (WBAN) to detect and intervene on physical activity in real-time for overweight youth.

E. Todd Schroeder received the B.S. in Human Physiology from the University of California at Davis in 1992, the Ph.D. in Biokinesiology from the University of Southern California (Clinical Exercise Physiology), Los Angeles, CA in 2000.
He is currently an Assistant Professor of Clinical Physical Therapy at the Division of Biokinesiology and Physical Therapy, University of Southern California, Los Angeles, CA. His primary research interest is in the mechanisms whereby progressive resistance training and testosterone treatment stimulate protein synthesis and improve muscle quality in older persons. Additional research interests include understanding the mechanisms (signals/factors) associated with eccentric resistance exercise that induces hypertrophic adaptations and the implications of such exercise in older individuals to optimize rehabilitation.

Donna Spruijt-Metz received the B.S. degree in Psychology from the University of Amsterdam, The Netherlands in 1986, the M.S. degree in Psychology (Research Methods) from the University of Amsterdam, The Netherlands in 1991 and the Ph.D. in Adolescent Health/Medical Ethics from the Free University, Amsterdam, The Netherlands in 1996.
She is currently an Associate Professor of Research at the Department of Preventive Medicine, Keck School of Medicine. Her research focuses on pediatric obesity, human motivation and adolescent health, particularly in the areas of diet and physical activity. Current research includes a longitudinal study of the impact of puberty on insulin dynamics, mood and physical activity in African American and Latina girls, and an in-lab feeding study to determine the acute effects of high sugar meals on physical activity and other metabolic outcomes in African American and Latino youth.

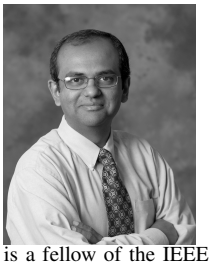

Gaurav S. Sukhatme received the B. Tech. degree in Computer Science and Engineering from the Indian Institute of Technology Bombay, Mumbai, India and the M.S. and Ph.D. degrees in Computer Science from USC.
He is a Professor of Computer Science (joint appointment in Electrical Engineering) at the University of Southern California (USC). He is the co-director of the USC Robotics Research Laboratory and the director of the USC Robotic Embedded Systems Laboratory which he founded in 2000. He is a fellow of the IEEE and a recipient of the NSF CAREER award and the Okawa foundation research award. He is the Editor-in-Chief of Autonomous Robots and has served as Associate Editor of the IEEE Transactions on Robotics and Automation, the IEEE Transactions on Mobile Computing, and on the editorial board of IEEE Pervasive Computing.